Appendix E

Online Selection

E.1 Introduction

The CMS trigger menu depends upon the luminosity delivered by the LHC and the available bandwidth between and out of the systems. The LHC luminosity is expected to start at $\mathcal{L} = 10^{32}\,\mathrm{cm}^{-2}\,\mathrm{s}^{-1}$ in 2007 and gradually rise to $\mathcal{L} = 10^{34}\,\mathrm{cm}^{-2}\,\mathrm{s}^{-1}$ by 2010. The CMS data acquisition can be operated with one to eight slices of Event Filter Farms that execute High-Level Trigger (HLT) algorithms. It is expected that we start with one slice in 2007, allowing a bandwidth of 12.5 kHz between Level-1 and HLT, and build up to the full eight slices by 2010, when the Level-1 to HLT bandwidth can be raised to 100 kHz. It is assumed that the data logging capability after the HLT selection will remain constant at a rate between 100 Hz to 150 Hz*. The Level-1 and HLT algorithms will be configured to operate with the lowest possible thresholds making the best use of the available bandwidth.

Here we focus solely on trigger studies for $\mathcal{L} = 2 \times 10^{33}\,\mathrm{cm}^{-2}\,\mathrm{s}^{-1}$. The scenario of operation assumes that CMS uses four DAQ slices capable of 50 kHz. While the actual choice of trigger thresholds, especially at HLT, depends strongly upon the physics of interest at the time of operation, we propose here an example set of trigger menus within the constraints of the data acquisition system. An effort has been made to optimise the Level-1 and HLT thresholds coherently, taking into account possible bandwidth limitations.

The structure of this note is as follows: first we overview the object-identification algorithms used for these studies. The emphasis is given to the changes that have been introduced since a similar study was performed in the DAQ TDR [75]. We then introduce a series of new trigger paths, aiming at increasing the event yield for various physics analyses. The central idea is to exploit various multi-object (or *cross-channel*) triggers in an attempt to improve the rejection and, at the same time, lower the kinematic thresholds of the corresponding objects. We finally present the performance of the triggers, and we calculate the overlap among them and the total HLT output rate.

E.2 Description of trigger tools

E.2.1 Level-1 reconstruction

There have been no significant changes in the Level-1 algorithms since the DAQ TDR. We have introduced an H_{T} algorithm which sums the corrected jet E_{T} of all the jets found above

*At the time of the writing of this document, several scenarios for the HLT output rate, the disk requirements for the storage manager and the associated cost are under discussion.

a programmable threshold, within $|\eta| < 5$. It does not account for E_{T} carried by muons and neutrinos.

The Level-1 strategy is the following: We have made an effort to keep the thresholds at the same levels, or even reduce them in order to be able to study cross-channel triggers (typically appearing with lower kinematic cuts). The notable exception is the tau triggers, where an increase in the HCAL noise and the usage of a new pile-up model in the simulation do affect the Level-1 τ identification tools, and therefore the related trigger rates. We have introduced additional Level-1 conditions for all HLT paths. The determination of thresholds and prescales is a compromise between the desire to distribute reasonably the available L1 bandwidth to the various triggers, and the need to optimise the L1 and HLT thresholds coherently in well-defined trigger paths.

E.2.2 HLT reconstruction

Well defined Level-1 terms are used in order to obtain triggers whose behaviour and efficiency can be studied with real data. We have replaced some of the Level-1 conditions with respect to the DAQ TDR with new Level-1 terms when this leads to more reasonable trigger paths or triggers that are more stable and carry less of a bias. The optimisation of the thresholds for the various triggers has been a compromise between the physics needs of the CMS experiment and the total HLT rate available. This study serves only as an intermediate step in a long-term trigger study project. Further improvements in the reconstruction tools, better optimisation of the thresholds, implementation of additional triggers and a CMS-wide discussion of the allocation of the HLT bandwidth to the physics groups according to the priorities of the experiment, are foreseen.

A general and detailed description of the HLT system can be found in Ref. [75]. Here we summarise the recent modifications of the HLT tools, and the expected changes in the rates of the various triggers with respect to the earlier studies.

- Muons: The muon algorithm has not changed, with the exception of the drift-tube local reconstruction and segment building. Therefore, no significant changes in the rates of single- and dimuon trigger paths are expected. The option of constructing muon triggers without isolation has been added.
- Electrons-Photons: Here the most important change is that all saturated trigger towers at Level-1 are now considered isolated. This increases both the signal efficiency and the background. At HLT, the photon rate can be reduced by increasing the thresholds or by applying some isolation cuts. For the electrons the options include a matching with pixel lines and tracks, as well as isolation requirements in the hadron calorimeter and the tracker. A study of the algorithm optimisation can be found in Ref. [7]. An improvement of the rejection power of the electron-photon algorithms is achieved with a simultaneous decrease of the HLT thresholds. Similar enhancements are expected for cross-channel triggers where one of the objects under consideration is an electron or a photon.
- Jets and $E_{\mathrm{T}}^{\mathrm{miss}}$: The main jet-finder algorithm (Iterative Cone with $R = 0.5$) has not been modified. Some optimisations of the tower thresholds have been added, and the jet corrections have been updated ("Scheme C"). Similarly, there are no major algorithm changes for $E_{\mathrm{T}}^{\mathrm{miss}}$, however it has been ensured that all triggers including a $E_{\mathrm{T}}^{\mathrm{miss}}$ object do not have any off-line corrections applied. Another improvement that has been recently introduced is the ability to construct *acoplanar*

triggers by combining two jets, or a jet and a $E_{\mathrm{T}}^{\mathrm{miss}}$ object that do not lie "back-to-back". Details of the physics algorithms can be found in Refs. [164] and [147].

- b-jets: The algorithm now uses muon information for fast rejection. Further improvements have been made for faster decisions and for an increased efficiency in fully hadronic final states. The documentation for the b-jet HLT algorithm can be found in Ref. [289].
- Taus: The HLT τ algorithm has not changed. However, the increase in the Level-1 rate does propagate into the HLT. The isolation parameters for the electromagnetic calorimeter and the tracker have been tuned after recent studies performed by the Higgs group, described in Ref. [279]. The overall rate for τ-related triggers is expected to be slightly increased.

A new addition to the HLT reconstruction tools is the H_{T} algorithm. It sums the corrected jet E_{T} of all the $E_{\mathrm{T}} > 5\,\mathrm{GeV}$ jets found within $|\eta| < 5$, along with the energy of the $p_{\mathrm{T}} > 5\,\mathrm{GeV/c}$ HLT muons found in the event, and the $E_{\mathrm{T}}^{\mathrm{miss}}$ computed using the calorimeter deposits. It is meant to be driven off the corresponding L1 H_{T} term.

E.3 Triggering with forward detectors

E.3.1 Objective

We discuss [†] the feasibility of a special forward detectors trigger stream, with target output rate of $\mathcal{O}(1)$ kHz at L1 and $\mathcal{O}(1)$ Hz on the HLT, as well as the potential of the already foreseen CMS L1 trigger streams for retaining events with diffractive processes.

The proposed forward detectors trigger stream combines the information of the central CMS detector with that from detectors further downstream of the CMS IP. The forward detectors considered are the TOTEM T1 and T2 tracker telescopes as well as the TOTEM Roman Pot (RP) detectors up to 220 m downstream of CMS [822, 823]. Information from TOTEM will be available to the CMS L1 trigger. We also consider detectors at a distance of 420 m, in the cryogenic region of the LHC ring, currently being studied by the FP420 project [253].

Topologically, diffractive events are characterised by a gap in the rapidity distribution of final-state hadrons. In addition, the fractional momentum loss, ξ, of diffractively scattered protons peaks at $\xi = 0$ ("diffractive peak"). The TOTEM RP detectors will permit to measure protons in the region $0.2 > \xi > 0.02$. Detectors at a distance of 420 m from the IP would provide a coverage of $0.02 > \xi > 0.002$, complementary to that of the TOTEM detectors, but cannot be included in the Level-1 trigger without an increase in the Level-1 latency of 3.2 μs (though a special, long latency running mode might be feasible at lower luminosities).

The studies discussed in the following assume that the RP detectors are 100% efficient in detecting all particles that emerge at a distance of at least $10\,\sigma_{\mathrm{beam}} + 0.5$ mm from the beam axis (1.3 mm at 220 m, 4 mm at 420 m). Their acceptance was calculated for the nominal LHC optics ($\beta^* = 0.55$ m), version V6.5 [824, 825], and by way of a simulation program that tracks particles through the accelerator lattice [826]. LHC bunches with 25 ns spacing were assumed.

The results presented below do not depend on the specific hardware implementation of the TOTEM T1, T2 and RP detectors; they hold for any tracker system with the T1, T2 η coverage

[†] These studies were carried out in collaboration with TOTEM.

in conjunction with RPs at 220 m from the IP.

E.3.2 Level-1 trigger rates for forward detectors trigger stream

E.3.2.1 2-Jet conditions

A particularly interesting and challenging diffractive channel is the central exclusive production of a Higgs Boson, $pp \to pHp$, with Higgs mass close to the current exclusion limit. The dominant decay of a SM Higgs Boson of mass $\sim$120 GeV/c^2 is into two b-quarks and generates 2 jets with at most 60 GeV/c transverse momentum each. In order to retain as large a signal fraction as possible, as low an E_{T} threshold as possible of the Level-1 2-jet trigger is desirable. In practice, the threshold value cannot be chosen much lower than 40 GeV per jet. The Level-1 trigger applies cuts on the calibrated E_{T} value of the jet. Thus, a threshold of 40 GeV corresponds to 20-25 GeV in reconstructed E_{T}, i.e. to values where noise starts becoming sizable.

For luminosities of $10^{32}\,\mathrm{cm}^{-2}\,\mathrm{s}^{-1}$ and above, the Level-1 rate from standard QCD processes for events with at least 2 central jets ($|\eta| < 2.5$) with $E_{\mathrm{T}} > 40\,\mathrm{GeV}$ exceeds by far the target output rate of $\mathcal{O}(1)$ kHz. Thus additional conditions need to be employed to reduce the rate from QCD processes. The efficacy of several conditions was investigated [246, 247, 827–829]. In the following, the corresponding rate reduction factors are always quoted with respect to the rate of QCD events that contain at least 2 central jets with $E_{\mathrm{T}} > 40\,\mathrm{GeV}$ per jet.

The QCD background events were generated with the Pythia Monte Carlo generator. In order to assess the effect when the signal is overlaid with pile-up, a sample of 500,000 pile-up events was generated with Pythia. This sample includes inelastic as well as elastic and single diffractive events. Pythia underestimates the number of final state protons in this sample. The correction to the Pythia leading proton spectrum described in [830] was used to obtain the results discussed in the following.

Table E.1: Reduction of the rate from standard QCD processes for events with at least 2 central Level-1 jets with $E_T > 40\,\mathrm{GeV}$, achievable with requirements on the tracks seen in the RP detectors. Additional rate reductions can be achieved with the H_{T} condition and with a topological condition. Each of them yields, for all luminosities listed, an additional reduction by about a factor 2.

Luminosity [$\mathrm{cm}^{-2}\,\mathrm{s}^{-1}$]	Pile-up events per BX	Level-1 2-jet rate [kHz] for $E_{\mathrm{T}} >$ 40GeV	Total reduction needed	Reduction when requiring track in RPs at					
				220 m		420 m	220 & 420 m (asymmetric)		420 & 420 m
					$\xi < 0.1$			$\xi < 0.1$	
1×10^{32}	0	2.6	2	370					
1×10^{33}	3.5	26	20	7	15	27	160	380	500
2×10^{33}	7	52	40	4	10	14	80	190	150
5×10^{33}	17.5	130	100	3	5	6	32	75	30
1×10^{34}	35	260	200	2	3	4	17	39	10

Given a Level-1 target rate for events with 2 central Level-1 jets of $\mathcal{O}(1)$ kHz, a total rate reduction between a factor 20 at $1 \times 10^{33}\,\mathrm{cm}^{-2}\,\mathrm{s}^{-1}$ and 200 at $1 \times 10^{34}\,\mathrm{cm}^{-2}\,\mathrm{s}^{-1}$ is necessary. Table E.1 summarises the situation for luminosities between $10^{32}\,\mathrm{cm}^{-2}\,\mathrm{s}^{-1}$ and $10^{34}\,\mathrm{cm}^{-2}\,\mathrm{s}^{-1}$, and for different RP detector conditions: a track at 220 m on one side of the IP (single-arm

220 m), without and with a cut on ξ; a track at 420 m on one side of the IP (single-arm 420 m); a track at 220 m and 420 m (asymmetric); a track at 420 m on both sides of the IP (double-arm 420 m). Because the detectors at 220 m and 420 m have complementary coverage in ξ, the asymmetric condition in effect selects events with two tracks of very different ξ value, in which one track is seen at 220 m on one side of the IP and a second track is seen on the other side at 420 m. If not by the L1 trigger, these asymmetric events can be selected by the HLT and are thus of highest interest. At luminosities where pile-up is present, the rate reduction achievable with the RP detector conditions decreases because of the diffractive component in the pile-up.

A collimator located in front of the LHC magnet Q5, planned to be operative at higher luminosities, will have an effect on the acceptance of the RP detectors resembling that of a ξ cut. This effect has not been taken into account in Table E.1.

Using T1 and T2 as vetoes in events with 2 central Level-1 jets was found to be effective only in the absence of pile-up [831].

In addition to the E_{T} values of individual Level-1 jets, the CMS Calorimeter Trigger has at its disposal the scalar sum, H_{T}, of the E_{T} values of all jets. Requiring that essentially all the E_{T} be concentrated in the two central Level-1 jets with highest E_{T}, i.e. $[E_{\mathrm{T}}^{1} + E_{\mathrm{T}}^{2}]/H_{\mathrm{T}} > 0.9$ (H_{T} condition), corresponds to imposing a rapidity gap of at least 2.5 units with respect to the beam direction. This condition reduces the rate of QCD events by approximately a factor 2, independent of the presence of pile-up and with only a small effect on the signal efficiency.

A further reduction of the QCD rate could be achieved with the help of a topological condition. The 2-jet system has to balance the total momentum component of the two protons along the beam axis. In signal events with asymmetric ξ values, the proton seen on one side in the RP detectors at 220 m distance is the one with the larger ξ and thus has lost more of its initial momentum component along the beam axis. Hence the jets tend to be located in the same η-hemisphere as the RP detectors that detect this proton. A trigger condition requiring that $[\eta^{jet1} + \eta^{jet2}] \times \mathrm{sign}(\eta^{220m\ RP}) > 0$ reduces the QCD background by a factor 2, independent of pile-up, and with no loss in signal efficiency.

A reduction of the QCD rate to levels compatible with a Level-1 output target rate of $\mathcal{O}(1)$ kHz by including RP detectors at a distance of 220 m from the CMS IP thus appears feasible for luminosities up to $2 \times 10^{33}\,\mathrm{cm}^{-2}\,\mathrm{s}^{-1}$, as long as a ξ cut can be administered in the L1 trigger.

E.3.2.2 Other conditions

The effect of combining already foreseen Level-1 trigger conditions with conditions on the RP detectors is illustrated in Table E.2 [828]. Single- and double-arm RP detector conditions are indicated with 's' and 'd' endings, respectively. Entries marked with a '(c)' indicate thresholds applicable if a cut on $\xi < 0.1$ is implemented for the RP detectors at 220 m. The jet conditions consider all Level-1 jets with $|\,\eta\,| < 5$.

A further rate reduction by approximately a factor two can be obtained at luminosities with negligible pile-up by imposing a rough large rapidity gap cut at L1. This was implemented by requiring that there be no forward jets, i.e. jets in the HF, in either hemisphere in the event.

Table E.2: Estimated threshold values that result in a L1 output rate of ~ 1 kHz, for various conditions on central CMS detector quantities and on tracks seen in the RP detectors at 220 m and 420 m.

L1 condition	L1 E_{T} or p_{T} threshold [GeV] at $\mathcal{O}(1)$ kHz L1 output rate for luminosity [cm^{-2} s^{-1}]			
	1×10^{33}	2×10^{33}	5×10^{33}	1×10^{34}
1 Jet	115	135	160	190
2 Jet	90	105	130	150
1 Jet+220s	90	115	155	190
2 Jet+220s	65	90	125	150
1 Jet+220d	55	85	130	175
2 Jet+220d	30	60	100	140
1 Jet+220s(c)	70	90	150	185
2 Jet+220s(c)	60	70	115	145
1 Jet+220d(c)	30	65	110	155
2 Jet+220d(c)	20	45	85	125
1 Jet+420s	65	90	125	165
2 Jet+420s	45	70	100	130
1 Jet+420d	20	40	80	115
2 Jet+420d	< 10	30	60	90
1 μ+220s	12	16	23	> 100
1 μ+220d	4	9	17	80
1 μ+220s(c)	–	11	22	100
1 μ+220d(c)	–	6	13	30
1 μ+420s	7	11	14	37
1 μ+420d	< 2	4	7	14

E.3.3 Level-1 signal efficiencies

Of the Level-1 conditions discussed so far, only those based on the RP detectors have a significant impact on the signal efficiency. Of further interest is the question how many signal events are being retained by the already foreseen trigger streams, notably the muon trigger.

E.3.3.1 Central exclusive Higgs production ($H(120\,\mathrm{GeV/c^2}) \to b\bar{b}$)

In order to study the effect of the Level-1 trigger selection on the Higgs signal, signal samples of 100,000 events with central exclusive production of a Higgs Boson were generated with the Monte Carlo programs EDDE [260] (version 1.1) and Exhume [258] (version 1.0).

Figure E.1 shows the Level-1 selection efficiency as a function of the E_{T} threshold values when at least 2 central Level-1 jets with E_{T} above threshold are required [828]. For a threshold of 40 GeV per jet, Exhume and EDDE both yield an efficiency of about 20%. The plot on the right-hand side overlays the efficiency curves obtained with Exhume when the 2-jet condition is combines with RP detector conditions. With an E_{T} threshold of 40 GeV per jet, the single-arm 220 m (420 m) condition results in an efficiency of the order 12% (15%), the double-arm 420 m condition in one of 8% and the asymmetric condition in one of 6%. This also means that, even without the possibility of including the RP detectors at 420 m from the CMS IP in the Level-1 trigger, 6% of the signal events can be triggered on with the single-arm 220 m condition, but will have a track also in the 420 m detectors that can be used in the HLT.

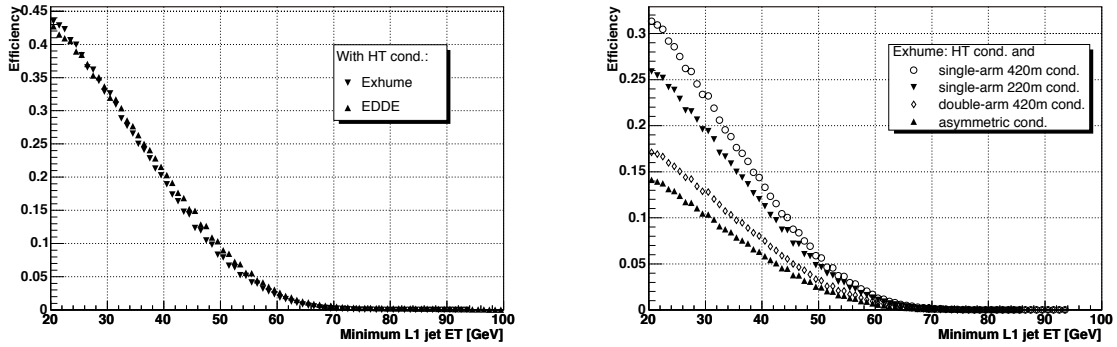

Figure E.1: L1 selection efficiency for $pp \to pHp$ and $H(120\,\text{GeV/c}^2) \to b\bar{b}$ as function of the E_T threshold value when at least 2 central Level-1 jets with E_T above threshold are required. All plots are for the non-pile-up case and the H_T condition has been applied. Left: Comparison between the EDDE and Exhume Monte Carlo generators, without applying any additional RP conditions. Right: Comparison of the effect of different RP conditions on the efficiency in the Exhume Monte Carlo sample.

An alternative trigger strategy is to exploit the relatively muon-rich final state from B-decays: about 20% of the events have at least a muon in the final state. Requiring at least one (two) L1 muon(s) with p_T above 14 GeV/c (3 GeV/c) yields an efficiency of 6% (2%). Demanding at least 1 muon and 1 jet, the latter with E_T >40 GeV, is a condition not yet foreseen in the CMS trigger tables. For a muon p_T threshold of 3 GeV/c, the rate at a luminosity of 10^{33} cm^{-2} is slightly less than 3 kHz, and about half of the decays with muons in the final state (*i.e.* 9 %) are retained [829].

E.3.3.2 Central exclusive Higgs production ($H(140\,\text{GeV/c}^2) \to WW$)

For SM Higgs Boson masses above 120 GeV/c^2, the $H \to WW$ branching ratio becomes sizable; in this case the final state contains high-p_T leptons that can be used for triggering. Efficiencies are in general high [829]. About 23% of the events have at least one muon in the final state. Approximately 70% of these (i.e. 16%) are retained by requiring at least one muon with a p_T threshold of 14 GeV/c. An extra $\approx 10\%$ (i.e. 2%) would be retained by implementing the muon/jet slot discussed above with thresholds of 3 GeV/c on the muon p_T and 40 GeV on the jet E_T.

E.3.3.3 Single diffractive hard processes

Double-Pomeron exchange processes constitute only a small part of the diffractive cross section. Hard single-diffraction, $pp \to pX$, where only one proton remains intact and the other is diffractively excited, have much higher cross sections than hard double-Pomeron exchange events. Efficiencies have been studied for $pp \to pX$, with X containing a W or a Z boson that decay to jets and to muons, as well as with X containing a dijet system. Samples of 100,000 signal events each were generated with the POMWIG Monte Carlo generator [832] (version 1.3).

For two example processes, Figure E.2 shows the efficiency as a function of the Level-1 threshold value, normalised to the number of events where for the diffractively scattered proton $0.001 < \xi < 0.2$ holds [828]. Three different trigger conditions are considered: trigger

on central detector quantities alone (i), trigger on central detector quantities in conjunction (ii) with the single-arm 220 m condition, and (iii) with the single-arm 420 m condition. Also shown is the number of events expected to pass the L1 selection per pb^{-1} of LHC running. A significant part of events is retained when a proton is required in the 220 m RPs.

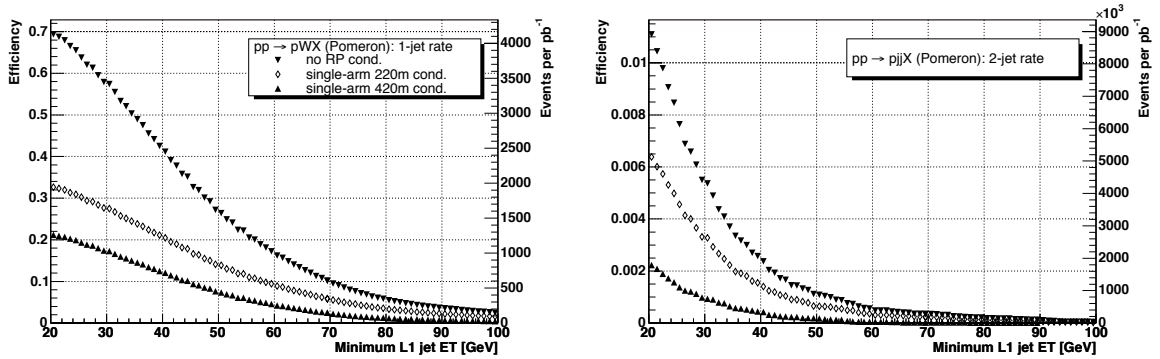

Figure E.2: L1 selection efficiency as function of the E_{T} threshold value for $pp \to pWX$ (left) and $pp \to pjjX$ (right), when at least one (left) or two (right) Level-1 jets ($|\eta| < 5$) above threshold are required. All plots are for the non-pile-up case.

E.3.4 Effect of pile-up, beam-halo and beam-gas backgrounds

Pile-up effects are included in all rate and efficiency studies presented. In the 220 m stations, 0.055 protons/pile-up event are expected on average, in the 420 m stations, 0.012 protons/pile-up event. At a luminosity of 10^{34} cm^{-2} s^{-1}, there are 35 pile-up events on average; this entails, on average, 2 extra tracks in the 220 m stations and less than one in the 420 m stations.

The effect from beam-halo and beam-gas events on the Level-1 rate is not yet included in the studies discussed here. Preliminary estimates suggest that they are chiefly a concern for any trigger condition based solely on the forward detectors. For any trigger condition that includes a requirement on central CMS detector quantities the size of their contribution is such that they do not lead to a significant increase of the Level-1 output rate.

E.3.5 HLT strategies

Jets are reconstructed at the HLT with an iterative cone ($R < 0.5$) algorithm. The Level-1 selection cuts are repeated with HLT quantities. The following conditions are imposed [828]:

- A The event pass the single-arm 220 m Level-1 condition with $\xi < 0.1$ cut. As demonstrated in Table E.1, this condition reduces the Level-1 output rate to below $\mathcal{O}(1)$ kHz. Additional rate reduction factors of ~ 300 (~ 1000) at $1(2) \times 10^{33}$ cm^{-2} s^{-1} are needed to reach the HLT target output rate of $\mathcal{O}(1)$ Hz.
- B The two jets are back-to-back in the azimuthal angle ϕ ($2.8 < \Delta\phi < 3.48$ rad), and have $(E_T^1 - E_T^2)/(E_T^1 + E_T^2) < 0.4$, and $E_T > 40$ GeV for each jet.
- C The proton fractional momentum loss ξ is evaluated with the help of calorimeter quantities [833–835]:

$$\xi_{+-} = (1/\sqrt{s})\Sigma_i E_{Ti} \exp(\mp\eta_i), \tag{E.1}$$

where the sum runs over the two jets and the $+, -$ signs denote the two hemispheres. The result is compared with the ξ value measured by the RP detectors. At present, no simulation of the RP reconstruction is available. As estimate of the ξ resolution, 15% (10%) is assumed at 220 m (420 m). Events are rejected if the difference between the two values of ξ is larger than $2\,\sigma$.

D At least one of the two jets is b-tagged.

E A proton is seen at 420 m.

The case without pile-up presents no difficulty: essentially no QCD background events survive the selection. If conditions A+B+C are applied, the signal efficiency for $pp \to pHp$ with $H(120\,\text{GeV/c}^2) \to b\bar{b}$ is at 11% essentially unchanged with respect to the Level-1 selection, but the HLT output rate exceeds the target output rate, see Table E.3. If b-tagging is required but no ξ matching (conditions A+B+D), the efficiency drops to 7%, without any improvement in the rate reduction. The combination of conditions A+B+C+E finally leads to the targeted HLT output rate of $\mathcal{O}(1)$ Hz, without any loss in signal efficiency compared to L1.

Table E.3: Results of HLT selection.

HLT selection condition	A+B+C	A+B+D	A+B+C+E
HLT rate at 1×10^{33} cm^{-2} s^{-1}	15 Hz	20 Hz	< 1 Hz
line HLT rate at 2×10^{33} cm^{-2} s^{-1}	60 Hz	80 Hz	1 Hz
e Signal eff. $H(120)\,\text{GeV/c}^2) \to b\bar{b}$	11%	7%	6 %

E.4 High-Level Trigger paths

We are starting with the DAQ-TDR trigger table as the baseline. This includes single- and double-triggers for the basic objects (e, γ, μ, τ) along with jets and b-jets. Some cross-channel triggers are also present. We are expanding the cross-channel "menu" by introducing additional triggers. We introduce an H_{T} algorithm, which we combine with other objects. We are also adding a series of central single-jets, non-isolated muons, and a diffractive trigger discussed earlier.

E.4.1 Level-1 conditions

Table E.4 summarises the Level-1 conditions used to drive all the trigger paths. A pseudo "L1 bit number" has been assigned for easy reference in the following sections.

E.4.2 Evolution of DAQ-TDR triggers

The trigger paths that have been studied in Ref. [75] have been inherited and constitute the "bulk" of this next iteration of the CMS Trigger Menu for $\mathcal{L} = 2 \times 10^{33}\,\text{cm}^{-2}\,\text{s}^{-1}$. Modifications (optimisation of isolation cuts and thresholds) have been made for certain of the triggers, to reflect changes in the physics algorithms, or the improved understanding of the background from Monte Carlo (MC) simulations. The proposed Trigger Tables includes:

- Muons: The standard muon triggers include calorimeter-based isolation at L2, and both calorimeter and tracker isolation at L3. The p_{T} thresholds remain at 19 GeV/c for the single-muon and (7, 7) GeV/c for the dimuon trigger. A second set of relaxed single- and double-muons has been added with $p_{\text{T}} > 37$ GeV and

Table E.4: Level-1 conditions used in High Level Trigger paths.

Level-1 bit #	Trigger	Thresholds (GeV)	Prescale
0	Single μ	14	1
1	Double μ	3	1
2	Single isolated $e\,\gamma$	23	1
3	Double isolated $e\,\gamma$	11	1
4	Double $e\,\gamma$ (isolated & non-isolated)	19	1
8	Single central jet	177	1
9	Single forward jet	177	1
10	Single τ-jet	100	1
11	2 central jets	130	1
12	2 forward jets	130	1
13	2 τ-jets	66	1
14	3 central jets	86	1
15	3 forward jets	86	1
16	3 τ-jets	40	1
17	4 central jets	70	1
18	4 forward jets	70	1
19	4 τ-jets	30	1
26	(isolated) $e\,\gamma$ + τ	14, 52	1
31	H_{T}	300	1
32	$E_{\mathrm{T}}^{\mathrm{miss}}$	60	1
33	Single jet (central, forward or τ)	140	10
34	Single jet (central, forward or τ)	60	1 000
35	Single jet (central, forward or τ)	20	100 000
36	Single jet (central, forward or τ)	150	1
37	2 jets (central, forward or τ)	100	1
38	3 jets (central, forward or τ)	70	1
39	4 jets (central, forward or τ)	50	1

$p_{\mathrm{T}} > 10\,\mathrm{GeV}$, respectively. The main motivation here is Drell-Yan studies. In general, physics analyses that do not need a low p_{T} muon but do suffer from the isolation requirement on the muon. The reduced rejection caused by the removal of the isolation cuts is compensated by the higher-p_{T} thresholds on the muons, without affecting the event yield for the physics signal. The relaxed triggers have the advantage that the muons here are immune to radiative losses for the higher energy spectrum ($p_{\mathrm{T}} > 500\,\mathrm{GeV/c}$). Both isolated and relaxed triggers run off the corresponding non-isolated single- and double-muon bits at L1.

- Electrons: The p_{T} threshold remains at 26 GeV/c for the single electron trigger and has a new value of (12, 12) GeV/c for the dielectron trigger. An additional relaxed dielectron trigger appears with $p_{\mathrm{T}} > 19\,\mathrm{GeV/c}$. The single-electron and double-electron triggers run off the corresponding Level-1 bits.
- Photons: The new p_{T} thresholds are 80 GeV/c for the single-photon trigger and (30, 20) GeV/c for the diphoton trigger (both relaxed and non-relaxed flavours). A few prescaled single- and double-photon triggers have also been introduced, for

the purpose of studying trigger efficiencies. The photon HLT algorithms run off the corresponding Level-1 $e\,\gamma$ bits (single- and double-triggers).

- Taus: The single-τ trigger runs off the corresponding Level-1 bit. The double-τ trigger is driven by the `.OR.`-ing of the single- and double-τ trigger bits at L1. There is no explicit kinematic cut on the tau at HLT. There is, however, a match-to-track requirement in addition to the $p_{\mathrm{T}} > 100$ (66) GeV/c L1 precondition for the inclusive (double) tau trigger. The single-τ has also a $E_{\mathrm{T}}^{\mathrm{miss}} > 65$ GeV requirement at HLT.
- Tau and electron: The Level-1 condition is the corresponding τ+$e\,\gamma$ trigger. The p_{T} threshold remains at 16 GeV/c for the electron. There is no explicit p_{T} cut for the τ at HLT, but there is the match-to-track requirement for the τ candidate.
- Jets: The Level-1 conditions for the single-, double-, triple- and quadruple-jet triggers have been simplified considerably. Single jet triggers run off an `.OR.` of a central-, forward- or tau-jet trigger at L1. Double-, triple- and quadruple-jet triggers use an `.OR.` of the all the Level-1 terms requiring the same number of jets or less. For example, the triple-jet trigger is driven by an `.OR.` of the single-, double- and triple-jet Level-1 bits. In all cases, jets can be found in either the central or the forward region of the detector, and they include the τ candidates. The additional p_{T} cuts at HLT are: 400 (single), 350 (double), 195 (triple) and 80 (quadruple) GeV. The new double-jet trigger is expected to have a large overlap with the single-jet trigger path. However, it is useful for testing the additional bias introduced by the requirement for a second jet in the event. A series of prescaled triggers have also been introduced, which are discussed later (Sec. E.4.3.2).
- b-jet: This trigger is also based on the logical `.OR.` of the single-, double-, triple- and quadruple-jet Level-1 terms. At HLT, we have the additional requirement that the event is consistent with b-content. The E_{T} cut for the HLT jets is one of the following: 350 GeV if the event has one jet, 150 GeV if the event has three jets, or 55 GeV if the event has four jets.
- Jet and $E_{\mathrm{T}}^{\mathrm{miss}}$: The E_{T} thresholds are 180 and 80 GeV, respectively. The Level-1 condition is a single $E_{\mathrm{T}}^{\mathrm{miss}}$ object above 60 GeV.

E.4.3 New triggers

E.4.3.1 Cross-channel triggers

The trigger studies presented in the DAQ TDR [75] have been the most comprehensive CMS effort to date to calculate rates for various trigger paths across many physics channels. For those studies the focus has been the optimisation of the rejection of the individual object-id algorithms (muon, electron, tau, etc.) rather than the combination of them into more powerful trigger tools. However, single (or even double) trigger objects are limited by the rate and, therefore, have their thresholds often higher than desired for many physics analyses. If the signal contains more than one trigger objects, using trigger paths combining different objects may yield a considerable gain by allowing lower trigger thresholds and higher efficiency. Cross-channel triggers can be much more stable and less prone to rate fluctuations from operating conditions. The correlations among trigger objects can help reduce difficult backgrounds and instrumental fakes. The additional advantage is that such cross-channel triggers have noticeably lower rates than the single trigger channels and therefore contribute fairly little to the overall bandwidth.

Some cross-channel triggers have already been considered and their rates estimated [75], such as τ + e and τ + $E_{\mathrm{T}}^{\mathrm{miss}}$, motivated by the Higgs searches with hadronic decays of τ and leptons, and jet + $E_{\mathrm{T}}^{\mathrm{miss}}$, important for searches of super-symmetric particles. The new addition to the Trigger Menu, expanding the scope of Higgs searches, is a combined τ + μ trigger with p_{T} thresholds at 40 and 15 GeV/c, respectively. It is driven by the single-μ Level-1 bit.

We are presenting here a few additional cross-channel triggers, along with the physics motivation.

- A new category of triggers introduced here is the acoplanar dijet and jet+$E_{\mathrm{T}}^{\mathrm{miss}}$ for SUSY signals. The gain is the lower thresholds that become possible because of the topology constraint. Possible biases should be studied, so these triggers are meant to run in parallel with the standard jet and jet + $E_{\mathrm{T}}^{\mathrm{miss}}$ triggers without the acoplanarity requirements. We introduce a double-jet trigger with E_{T} thresholds at (200, 200) GeV and $|\Delta\phi| < 2.1$, and a new Jet + $E_{\mathrm{T}}^{\mathrm{miss}}$ trigger with E_{T} thresholds at (100, 80) GeV and $|\Delta\phi| < 2.1$. The former is driven by an `.OR.` of the single- and double-jet requirements at Level-1 (bits 36, 37). The latter is driven by a simple $E_{\mathrm{T}}^{\mathrm{miss}} > 60$ GeV Level-1 requirement.
- "$E_{\mathrm{T}}^{\mathrm{miss}} + X$" triggers: A combination of an $E_{\mathrm{T}}^{\mathrm{miss}}$ object with an H_{T} cut, one (or more) jet or lepton may be the only way to access $E_{\mathrm{T}}^{\mathrm{miss}}$-enhanced triggers if there are problems (*e.g.* instrumental fakes) that prevent CMS from running an inclusive $E_{\mathrm{T}}^{\mathrm{miss}}$ trigger. At this point we have implemented:
  - Multi-jets and $E_{\mathrm{T}}^{\mathrm{miss}}$: These will be useful for SUSY studies, just like the series of jet triggers. However, the additional $E_{\mathrm{T}}^{\mathrm{miss}}$ requirement allows us to lower the thresholds on the jets, and therefore increase the sensitivity of the analyses. We introduce here a dijet + $E_{\mathrm{T}}^{\mathrm{miss}}$ trigger with $E_{\mathrm{T}}^{\mathrm{jet}} > 155$ GeV, $E_{\mathrm{T}}^{\mathrm{miss}} > 80$ GeV, a triple-jet + $E_{\mathrm{T}}^{\mathrm{miss}}$ trigger with $E_{\mathrm{T}}^{\mathrm{jet}} > 85$ GeV, $E_{\mathrm{T}}^{\mathrm{miss}} > 80$ GeV and a quadruple-jet + $E_{\mathrm{T}}^{\mathrm{miss}}$ trigger with $E_{\mathrm{T}}^{\mathrm{jet}} > 35$ GeV, $E_{\mathrm{T}}^{\mathrm{miss}} > 80$ GeV. These all run off the single Level-1 requirement for $E_{\mathrm{T}}^{\mathrm{miss}} > 60$ GeV.
  - H_{T} + $E_{\mathrm{T}}^{\mathrm{miss}}$ and H_{T} + e: It is difficult to contain the rate for an inclusive H_{T} trigger without any additional cuts. The requirement for a $E_{\mathrm{T}}^{\mathrm{miss}}$ cut or an additional electron in the event allows us to access events with lower $E_{\mathrm{T}}^{\mathrm{miss}}$ or softer electrons. This can give an increased efficiency for W+jets, top physics, SUSY cascades, and other similar physics channels. Here we propose an H_{T} + $E_{\mathrm{T}}^{\mathrm{miss}}$ trigger with $H_{\mathrm{T}} > 350$ GeV, $E_{\mathrm{T}}^{\mathrm{miss}} > 80$ GeV and an H_{T} + e trigger with $H_{\mathrm{T}} > 350$ GeV and $p_{\mathrm{T}} > 20$ GeV/c for the electron. They are both driven by the $E_{\mathrm{T}}^{\mathrm{miss}} > 60$ GeV condition at L1.

Some additional cross-channel triggers that have not been included in this Trigger Table iteration but should be considered in future trigger studies are

- An $e + \mu$ trigger is of interest in many studies, for example:
  - $qqH, H \rightarrow \tau\tau \rightarrow 2\ell$, with an expected gain thanks to the lower lepton thresholds compared to the single-electron and single-muon trigger paths,
  - many SUSY decays including leptons in the final state,

  - top measurements in the double leptonic channel ($t\bar{t} \to b\bar{b}\ell\nu\ell\nu$), gaining sensitivity at the lower p_{T} spectrum, and
  - $B_s \to \ell\ell$, to allow for the lepton-number-violating channel to be studied.
- $E_{\mathrm{T}}^{\mathrm{miss}} + \ell$: The idea here is to exploit the presence of a W boson or a top decay in many channels. This could be used in many SM channels where lowering the lepton threshold extends the range of the measurement. For example:
  - top measurement in the double leptonic and semi-leptonic channels,
  - single top production, and
  - W measurements.

  Furthermore, this is a typical signature of an event containing super-symmetric particles.
- Triggers combining a lepton and a jet, or a lepton and a $b-$jet could be of interest for top measurements. The ℓ + jet signature is also very common in supersymmetric events.
- Finally, a combination of a lepton and a photon ($e+\gamma$ and $\mu+\gamma$) is ideal for Flavour Changing Neutral Current analyses, exploiting the extraordinary capabilities of CMS in detecting photons. These triggers allow to lower the thresholds on the lepton and the photon, increasing the event yield compared to the single-e, μ or γ trigger paths.

E.4.3.2 Single-jet triggers

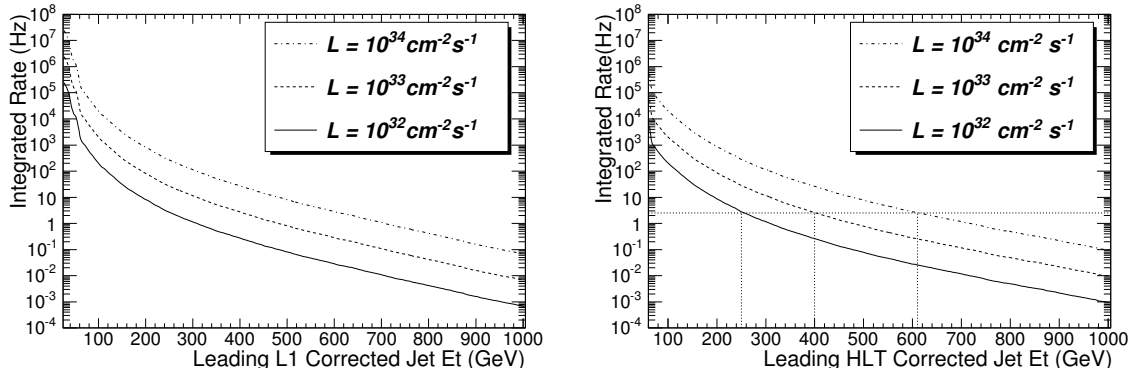

Figure E.3: The integrated trigger rates at Level-1 (left) and HLT (right) above the E_{T} thresholds for the highest E_{T} jet is plotted versus the E_{T} threshold for three luminosity scenarios: $\mathcal{L} = 10^{32}\,\mathrm{cm}^{-2}\,\mathrm{s}^{-1}$ (solid), and $\mathcal{L} = 10^{33}\,\mathrm{cm}^{-2}\,\mathrm{s}^{-1}$ (dashed), and $\mathcal{L} = 10^{34}\,\mathrm{cm}^{-2}\,\mathrm{s}^{-1}$ (dot-dashed). HLT thresholds that give 2.5 Hz are shown by vertical dotted lines.

In this section we describe the single jet trigger paths. These have been driven by the needs of the inclusive jet and dijet analysis. The full study can be found in Ref. [117]. Here we summarise the conclusions, along with a short description of the strategy for adjusting thresholds and prescales as the luminosity changes. This study looks at the evolution of the single-jet triggers for various luminosities. It serves as an example of how to preserve the long-term continuity of the triggers used for physics analyses. It is, therefore, interesting and instructive beyond the strict scope of the single-jet trigger suite.

To measure jet spectra down to low jet E_{T} and dijet mass requires multiple triggers, of roughly equal total rate, and with appropriately chosen E_{T} thresholds and prescales. In Fig. E.3 we show estimates of the Level-1 and HLT single jet trigger rates vs. corrected jet E_{T}. In Table E.5 we show the single jet trigger paths from Level-1 to HLT including thresholds, prescales and estimates of the rates. We find that the maximum allowed HLT rate is the constraining factor for triggering on jets. For luminosities $\mathcal{L} = 10^{32}\,\mathrm{cm}^{-2}\,\mathrm{s}^{-1}$, $\mathcal{L} = 10^{33}\,\mathrm{cm}^{-2}\,\mathrm{s}^{-1}$ and $\mathcal{L} = 10^{34}\,\mathrm{cm}^{-2}\,\mathrm{s}^{-1}$ the highest E_{T} threshold at HLT was chosen to give a rate of roughly 2.5 Hz, as illustrated in Fig. E.3, so that four triggers would saturate an allowed jet rate of roughly 10 Hz at HLT.

The highest E_{T} threshold at any luminosity is never prescaled. Lower thresholds are prescaled and are chosen at roughly half the E_{T} of the next highest threshold. This allows reasonable statistics in the overlap between the two samples, necessary for measuring trigger efficiencies and producing a continuous jet spectrum. The total Level-1 jet rate required is only around 0.3 kHz, a small fraction of the L1 total bandwidth. Since these triggers are limited by HLT, not L1, for each trigger path the Level-1 thresholds are chosen low enough to have a L1 trigger efficiency of more than 95% at the corresponding HLT threshold in the path, as shown in Fig. E.4. This strategy utilises ten times more bandwidth at Level-1 than at HLT to insure that all of the resulting HLT sample has high enough trigger efficiency to be useful for analysis.

Table E.5: Single jet trigger table showing path names, trigger thresholds in corrected E_{T}, prescales, and estimated rates at L1 and HLT for four different luminosity scenarios.

Path	L1				HLT	
	E_{T} Cut (GeV)	Unpres. Rate (KHz)	Prescale (N)	Presc. Rate (kHz)	E_{T} Cut GeV)	Rate (Hz)
Single Jet Triggers in Scenario 1: $\mathcal{L} = 10^{32}\,\mathrm{cm}^{-2}\,\mathrm{s}^{-1}$						
High	140	0.044	1	0.044	250	2.8
Med	60	3.9	40	0.097	120	2.4
Low	25	2.9×10^2	2,000	0.146	60	2.8
Single Jet Triggers in Scenario 2: $\mathcal{L} = 10^{33}\,\mathrm{cm}^{-2}\,\mathrm{s}^{-1}$						
Ultra	270	0.019	1	0.019	400	2.6
High	140	0.44	10	0.044	250	2.8
Med	60	39	400	0.097	120	2.4
Low	25	2.9×10^3	20,000	0.146	60	2.8
Single Jet Triggers in Scenario 3: $\mathcal{L} = 2 \times 10^{33}\,\mathrm{cm}^{-2}\,\mathrm{s}^{-1}$						
Ultra	270	0.038	1	0.038	400	5.2
High	140	0.88	20	0.044	250	2.8
Med	60	78	800	0.097	120	2.4
Low	25	5.8×10^3	40,000	0.146	60	2.8
Single Jet Triggers in Scenario 4: $\mathcal{L} = 10^{34}\,\mathrm{cm}^{-2}\,\mathrm{s}^{-1}$						
Super	450	0.014	1	0.014	600	2.8
Ultra	270	0.19	10	0.019	400	2.6
High	140	4.4	100	0.044	250	2.8
Med	60	3.9×10^2	4,000	0.097	120	2.4
Low	25	2.9×10^4	200,000	0.146	60	2.8

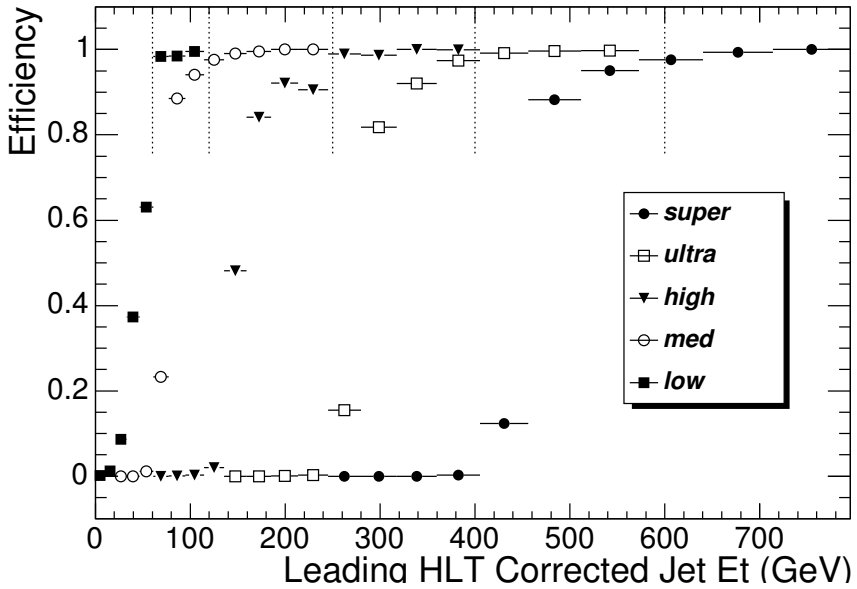

Figure E.4: The efficiency for passing the Level-1 jet trigger is shown as a function of HLT corrected jet E_T for each of the trigger paths shown in Table E.5. The Level-1 thresholds were chosen to give an efficiency of greater than 95% at the corresponding HLT threshold.

Table E.5 illustrates an example trigger strategy to maintain the continuity of jet analysis as the luminosity increases over a time span of years. The most important reason for introducing a series of multiple triggers with varying thresholds and prescales is the continuity of the trigger path for the physics analyses. For every new "luminosity era" CMS enters, it is fundamental that we maintain the thresholds introduced in the previous months or years, allowing combination of trigger samples over time. For the prescaled thresholds, we may increase the prescales, either in discrete steps or dynamically, to maintain the allowed HLT rate with increasing luminosity. However, to maintain maximum sensitivity to new physics, the highest E_{T} threshold must never be prescaled. For example, in Table E.5 when the luminosity increases by only a factor of 2 from $\mathcal{L} = 10^{33}\,\mathrm{cm}^{-2}\,\mathrm{s}^{-1}$ to $\mathcal{L} = 2 \times 10^{33}\,\mathrm{cm}^{-2}\,\mathrm{s}^{-1}$, we double the prescales on the lower-E_{T} triggers but don't change either the threshold or the prescale of the highest E_{T} trigger labelled Ultra. This allows us to maintain stability of the trigger thresholds, and analyses that depend on them, with only modest increases in the total rate for single object triggers. When the HLT rate in the unprescaled trigger becomes intolerably high, a higher E_{T} threshold unprescaled trigger is introduced, and the old unprescaled trigger can then be prescaled as necessary.

For the particular case of single-jet triggers: To commission the calorimeters, or perform a one-time jet study, it may be desirable to have more jets. If we want to write more than roughly 10 Hz of single jets at HLT, we can still use the same suite of single-jets, but lower the prescales to obtain more jets at low E_{T}. This is preferable to moving the threshold for the unprescaled trigger, or any of the triggers, and ending up with a special trigger that is only applicable for a given running period and difficult to combine with other samples.

For $\mathcal{L} = 2 \times 10^{33}\,\mathrm{cm}^{-2}\,\mathrm{s}^{-1}$, the suggested jet thresholds have been studied again in the scope of the global High-Level trigger analysis (Sec. E.5) and new Level-1 prescales and rates have

been determined. For the trigger table proposed in this study, we have chosen four triggers, with E_{T} thresholds of 400, 250, 120 and 60 GeV, and prescales of 1, 10, 1000 and 100 000, respectively.

E.4.3.3 Other triggers

The remaining triggers that have been introduced since the DAQ TDR are:

- Inclusive $E_{\mathrm{T}}^{\mathrm{miss}}$ trigger: As discussed earlier, this is a difficult trigger that is subject to the good understanding and control of the detector noise. We suggest here a single $E_{\mathrm{T}}^{\mathrm{miss}}$ trigger with $E_{\mathrm{T}} > 91$ GeV, driven by the $E_{\mathrm{T}}^{\mathrm{miss}} > 60$ GeV L1 condition. This is just an indicative value, rather on the low side, as $E_{\mathrm{T}}^{\mathrm{miss}}$ rates appear lower compared to Ref. [75]. It is foreseen that additional $E_{\mathrm{T}}^{\mathrm{miss}}$ triggers with different thresholds and prescales will be introduced in the future.
- Diffractive trigger: This trigger is different than all others described earlier in that it uses the TOTEM detector [822, 823]. At Level-1 we ask for two central jets with $E_{\mathrm{T}} > 40$ GeV , along with a proton tagged with the 220 m Roman Pot. At HLT, a similar dijet cut and a "back-to-back" azimuthal condition are applied. We also require that we have a consistent measurement of the proton energy loss ξ in the two hemispheres (within 2 σ, measured at the Roman Pots). A final condition for a tagged proton seen by the 420 m Roman Pot brings the HLT rate down to $\mathcal{O}(1)$ Hz. This trigger is discussed in detail in Sec. E.3.

E.5 Performance

The performance of the trigger system is studied by using simulated data that has been digitised with appropriate pileup[‡], taking into account both the inelastic (55.2 mb) and the diffractive (24.1 mb) cross sections. To reduce the amount of simulation time, about 50 million minimum bias events were simulated and reused in random combinations. It was ensured that these events do not cause triggers by themselves to avoid over estimating the rates due to this reuse of events.

In the following sections we list trigger rates along with their statistical uncertainties. These take into account the luminosity-dependent weight of the events from the different samples, the corresponding cross sections and the $\hat{p_{\mathrm{T}}}$ of the main interaction and the pile-up contribution. They do *not* take into account the uncertainties of these individual factors, *i.e.* no systematic effects are studied here.

The Level-1 calorimeter trigger object rate studies are performed using QCD data that has been generated in several bins of $\hat{p_{\mathrm{T}}}$. A special event-weighting procedure has been applied to properly take into account the cross sections of the sub-samples. The Level-1 muon and $E_{\mathrm{T}}^{\mathrm{miss}}$ rate studies are performed using a purely minimum bias sample.

The HLT rates are estimated using specially enriched samples. For the triggers invoking muons, electrons and photons we have used a minimum bias sample enriched in muons, as well as $W \longrightarrow e/\,\mu\,\nu$, $Z \longrightarrow ee/\,\mu\mu$ and jet(s) + γ MC datasets. For the triggers including jets we have used QCD samples. These samples also contribute to the electron and photon triggers. Events triggered exclusively with muons have been excluded from the QCD sam-

[‡]We have estimated the average number of in-time interactions per bunch crossing to be 5 for $\mathcal{L} = 2 \times 10^{33}\,\mathrm{cm}^{-2}\,\mathrm{s}^{-1}$. Additional, out-of-time interactions have been ignored.

ples, to avoid double-counting with the muon-enriched sample. Table E.6 summarises the MC samples used for the trigger studies, and their corresponding contribution to the HLT rate. A more detailed breakdown of the contributions to the electron, photon and muon trigger rates from the different samples is discussed later (Sec. E.5.3). For our calculations, we have used the standard HLT physics algorithms (`ORCA_8_13_3` [10]) for the implementation of all trigger paths. At the time of this writing, this includes the latest algorithms and jet calibrations. For the global evaluation of the trigger rates we have used the "HLT steering code"

E.5.1 Level-1 rates

The background at Level-1 is entirely dominated by strong interactions. The muon rates at Level-1 are dominated by low p_{T} muons which are reconstructed as high p_{T} muons due to limited resolution at the trigger level. For the electron/photon trigger the rate is dominated by jets that fragment to high E_{T} π^0s. The jet rates are dominated by true jets in the QCD events. The $E_{\mathrm{T}}^{\mathrm{miss}}$ background is due to the limited energy resolution, and pile-up of minimum bias interactions.

We first produce a trigger table with Level-1 rates for DAQ TDR chosen thresholds for comparison. For the calculations we use a sample of 2 million minimum bias crossings with an average of 5 events per crossing, constructed from the minbias events, without reuse of events. The out-of-time pile-up is neglected. Even though there are small differences for the individual triggers, the integral rate is consistent with the rates reported in Ref. [75]. This comparison serves as a cross-check and is a necessary intermediate step before the introduction of new trigger terms. Table E.7 summarises the Level-1 rate calculations for the DAQ TDR triggers with the new MC samples. Besides the "95% efficiency points" (used throughout the DAQ TDR), the applied L1 thresholds are also given.

For the new trigger table: We select several thresholds for each trigger object type and quote corresponding rates and prescales for $\mathcal{L} = 2 \times 10^{33}\,\mathrm{cm}^{-2}\,\mathrm{s}^{-1}$. For the single objects we have added a series of prescaled triggers to determine the efficiency turn-on. For the multi-object triggers we have picked the lowest common threshold that is allowed for the allocated bandwidth. For the cross-channel triggers we have attempted to keep the lepton thresholds as low as possible, within the allocated bandwidth based on the physics needs of the experiment. The prescales are chosen such that the simulated rate at all times falls below the DAQ bandwidth taking into account a safety factor of 3. The total Level-1 rate for all triggers (including prescaled ones) is 22.6 ± 0.3 kHz.

E.5.2 Level-1 trigger object corrections

The trigger decisions are based on E_{T} of the objects reconstructed by various algorithms. Unfortunately, the energy deposition in the calorimeter and the size of the trigger towers, are not entirely uniform. We have used fits to the reconstructed-to-generated E_{T} ratios to correct for non-uniformity of the response for jets and electron/photon candidates found at all levels of trigger [829]. This correction procedure adjusts the mean response to the generated level.

The energy response of the calorimeters and the limited number of bits used in trigger calculations result in a finite resolution for the reconstructed trigger objects. Similarly, misalignments of the tracking systems and the limited number of patterns in the muon trigger look-up-tables also result in a finite resolution. To avoid systematic problems in understand-

ing the trigger efficiency turn-on with the E_{T} of the trigger objects, it is envisioned that only data where high trigger efficiency is assured is used for analysis.

E.5.3 HLT rates

A rough comparison of the HLT bandwidth given to various triggers, calculated with the latest algorithms and the ones reported in Ref. [75] is shown in Table E.8. It must be noted that not only thresholds but also other cuts are different in the two trigger studies. Furthermore, additional changes in the HLT algorithms (summarised in Sec. E.2.2) must be taken into account. This comparison serves only as a consistency check. It reaffirms that despite the evolution of the CMS reconstruction algorithms over the years, trigger rates remain under control and that no major bandwidth changes are expected.

The contributions to the single and double electron and photon trigger rates at HLT from the various MC samples is given at Table E.9. The main contributions to the single electron trigger come from the QCD and $W \longrightarrow e\nu$ samples, whereas for the single photon trigger the primary source is the jet(s) + γ events.

Table E.10 shows in a similar way the contributions to the single and double standard and relaxed muon rates from the various MC samples.

E.5.4 Trigger tables

Table E.11 summarises the Level-1 triggers used in this study, their kinematic thresholds, the individual and cumulative rates. We have assumed a DAQ capability of 50 kHz, taking into account a safety factor of 3.

Table E.12 gives the full list of trigger paths proposed for $\mathcal{L} = 2 \times 10^{33}\,\mathrm{cm}^{-2}\,\mathrm{s}^{-1}$ that have been described earlier for an HLT output rate of approximately 120 Hz.

Fig. E.5 shows a graphic representation of the HLT bandwidth assigned to all trigger paths presented in this study. For the triggers that appeared in the DAQ TDR, the corresponding rates are overlaid, in a heuristic comparison.

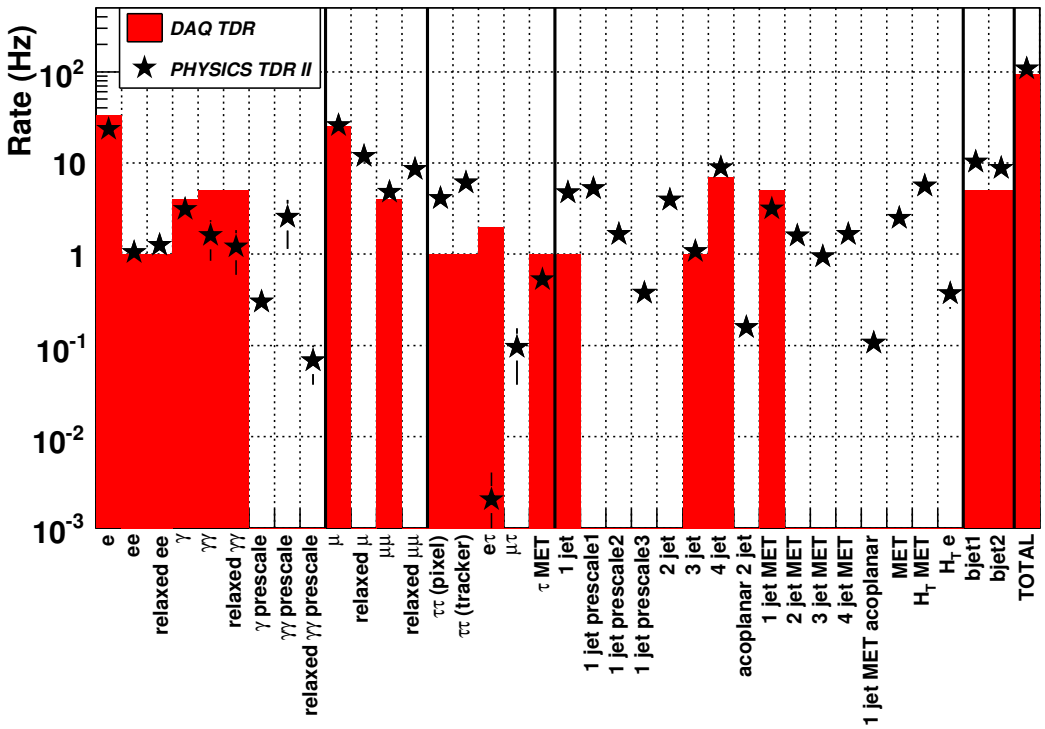

Figure E.5: Heuristic comparison of HLT bandwidth assigned to various trigger paths calculated in this study with the DAQ TDR. For the triggers introduced in this study the DAQ TDR entries appear empty. See text for details on different kinematic cuts and changes in the HLT algorithms.

Table E.6: Description and sizes of MC Samples used for the trigger studies. The contribution to the HLT rate does not include pre-scaled triggers.

Sample description	Cuts (Momenta in GeV/c)	Cross section (mb)	# of events	HLT rate (Hz)
Minimum bias with in-time pile-up; <# of interactions>= 5	—	79.3	50 000 000	—
QCD	$\hat{p_{\mathrm{T}}} \in [15, 20]$	1.46×10^{0}	49 491	
QCD	$\hat{p_{\mathrm{T}}} \in [20, 30]$	6.32×10^{-1}	49 244	
QCD	$\hat{p_{\mathrm{T}}} \in [30, 50]$	1.63×10^{-1}	49 742	
QCD	$\hat{p_{\mathrm{T}}} \in [50, 80]$	2.16×10^{-2}	99 486	
QCD	$\hat{p_{\mathrm{T}}} \in [80, 120]$	3.08×10^{-3}	96 238	
QCD	$\hat{p_{\mathrm{T}}} \in [120, 170]$	4.94×10^{-4}	99 736	
QCD	$\hat{p_{\mathrm{T}}} \in [170, 230]$	1.01×10^{-4}	99 226	
QCD	$\hat{p_{\mathrm{T}}} \in [230, 300]$	2.45×10^{-5}	99 481	
QCD	$\hat{p_{\mathrm{T}}} \in [300, 380]$	6.24×10^{-6}	98 739	
QCD	$\hat{p_{\mathrm{T}}} \in [380, 470]$	1.78×10^{-6}	46 491	
QCD	$\hat{p_{\mathrm{T}}} \in [470, 600]$	6.83×10^{-7}	47 496	
QCD	$\hat{p_{\mathrm{T}}} \in [600, 800]$	2.04×10^{-7}	48 986	
QCD	$\hat{p_{\mathrm{T}}} \in [800, 1000]$	3.51×10^{-8}	45 741	
Partial total			930 099	55.3 ± 6.9
$W \longrightarrow e\nu$	1 electron with $\lvert\eta\rvert < 2.7$, $p_{\mathrm{T}} > 25$	7.9×10^{-6}	3 944	9.7 ± 0.2
$Z \longrightarrow ee$	2 electrons with $\lvert\eta\rvert < 2.7$, $p_{\mathrm{T}} > 5$	8.2×10^{-7}	4 000	1.4 ± 0.0
$pp \longrightarrow \mathrm{jet(s)} + \gamma$, $\hat{p_{\mathrm{T}}} > 30\,\mathrm{GeV/c}$	jet: $p_{\mathrm{T}} > 20$, γ: $p_{\mathrm{T}} > 30$	2.5×10^{-6}	4 000	1.0 ± 0.0
$W \longrightarrow \mu\nu$	1 muon with $\lvert\eta\rvert < 2.5$, $p_{\mathrm{T}} > 14$	9.8×10^{-6}	4 000	14.0 ± 0.3
$Z \longrightarrow \mu\mu$	2 muons with $\lvert\eta\rvert < 2.5$, $p_{\mathrm{T}} > 20, 10$	7.9×10^{-7}	2 941	1.5 ± 0.0
$pp \longrightarrow \mu + X$	1 muon with $p_{\mathrm{T}} > 3$	2.4×10^{-2}	839 999	25.5 ± 1.2

Table E.7: Trigger table showing Level-1 rates for DAQ TDR chosen thresholds for $\mathcal{L} = 2 \times 10^{33}\,\mathrm{cm}^{-2}\,\mathrm{s}^{-1}$. Whenever the "95% efficiency point" is reported in DAQ TDR, we also give the actual kinematic threshold that has been applied.

Trigger	95% Eff. point	Threshold (GeV)	Rate (kHz)	Cumulative Rate (kHz)
Single $e\,\gamma$	29	23.4	3.38 ± 0.23	3.4 ± 0.2
Double $e\,\gamma$	17	11.5	0.85 ± 0.12	4.0 ± 0.3
Single μ	—	14	2.53 ± 0.20	6.5 ± 0.3
Double μ	—	3	4.05 ± 0.26	10.3 ± 0.4
Single τ	86	93	3.56 ± 0.24	9.7 ± 0.4
Double τ	59	66	1.97 ± 0.18	10.6 ± 0.4
1-, 3-, 4-jets	177, 86, 70	135, 58, 45	2.43 ± 0.20	11.9 ± 0.4
Jet + $E_{\mathrm{T}}^{\mathrm{miss}}$	—	88, 46	1.07 ± 0.13	12.2 ± 0.4
$e\,\gamma + \tau$	—	21, 45	3.64 ± 0.24	12.9 ± 0.5
Level-1 Trigger Total				12.9 ± 0.5

Table E.8: Comparison of HLT bandwidth given to various trigger paths calculated in this study with the DAQ TDR. See text for details on different kinematic cuts and changes in the HLT algorithms.

Trigger	DAQ TDR Rate (Hz)	New Rate (Hz)
Inclusive e	33.0	23.5 ± 6.7
e-e	1.0	1.0 ± 0.1
Relaxed e-e	1.0	1.3 ± 0.1
Inclusive γ	4.0	3.1 ± 0.2
γ-γ	5.0	1.6 ± 0.7
Relaxed γ-γ	5.0	1.2 ± 0.6
Inclusive μ	25.0	25.8 ± 0.8
μ-μ	4.0	4.8 ± 0.4
τ + $E_{\mathrm{T}}^{\mathrm{miss}}$	1.0	0.5 ± 0.1
τ + e	2.0	< 1.0
Double Pixel τ	1.0	4.1 ± 1.1
Double Tracker τ	1.0	6.0 ± 1.1
Single jet	1.0	4.8 ± 0.0
Triple jet	1.0	1.1 ± 0.0
Quadruple jet	7.0	8.9 ± 0.2
jet + $E_{\mathrm{T}}^{\mathrm{miss}}$	5.0	3.2 ± 0.1
b-jet (leading jet)	5.0	10.3 ± 0.3
b-jet (2^{nd} leading jet)	5.0	8.7 ± 0.3

Table E.9: Contributions to the HLT rates for the electron and photon triggers from the various MC datasets.

Trigger	Threshold (GeV)	Rates (Hz)			
		QCD	$W \longrightarrow e\nu$	$Z \longrightarrow ee$	jet(s) + γ
Inclusive e	26	12.6 ± 6.7	9.7 ± 0.2	1.2 ± 0.0	—
e-e	12, 12	0.1 ± 0.1	—	1.0 ± 0.0	—
Relaxed e-e	19, 19	0.3 ± 0.1	—	1.0 ± 0.0	—
Inclusive γ	80	1.1 ± 0.2	—	—	2.0 ± 0.1
γ-γ	30, 20	1.3 ± 0.8	—	—	0.3 ± 0.0
Relaxed γ-γ	30, 20	0.9 ± 0.6	—	—	0.3 ± 0.0

Table E.10: Contributions to the HLT rates for the muon triggers from the various MC datasets.

Trigger	Threshold (GeV)	Rates (Hz)		
		Enriched-μ sample	$W \longrightarrow \mu\nu$	$Z \longrightarrow \mu\mu$
Inclusive μ	19	10.9 ± 0.8	13.4 ± 0.3	1.5 ± 0.0
Relaxed μ	37	5.1 ± 0.5	5.7 ± 0.1	1.1 ± 0.0
μ-μ	7, 7	3.4 ± 0.4	—	1.3 ± 0.0
Relaxed μ-μ	10, 10	7.1 ± 0.5	—	1.4 ± 0.0

Table E.11: The Level-1 Trigger Menu at $\mathcal{L} = 2 \times 10^{33}\,\mathrm{cm}^{-2}\,\mathrm{s}^{-1}$ İndividual and cumulative rates are given for the different trigger paths and selected kinematic thresholds.

Trigger	**Level-1 Threshold (GeV)**	**Level-1 Rate (kHz)**	**Cumulative Level-1 Rate (kHz)**
Inclusive $e\,\gamma$	22	4.2 ± 0.1	4.2 ± 0.1
Double $e\,\gamma$	11	1.1 ± 0.1	5.1 ± 0.1
Inclusive μ	14	2.7 ± 0.1	7.8 ± 0.2
Double μ	3	3.8 ± 0.1	11.4 ± 0.2
Inclusive τ	100	1.9 ± 0.1	13.0 ± 0.2
Double τ	66	1.8 ± 0.1	14.1 ± 0.2
1-,2-,3-,4-jets	150,100,70,50	1.8 ± 0.1	14.8 ± 0.3
H_{T}	300	1.2 ± 0.1	15.0 ± 0.3
$E_{\mathrm{T}}^{\mathrm{miss}}$	60	0.3 ± 0.1	15.1 ± 0.3
H_{T} + $E_{\mathrm{T}}^{\mathrm{miss}}$	200, 40	0.7 ± 0.1	15.3 ± 0.3
jet + $E_{\mathrm{T}}^{\mathrm{miss}}$	100, 40	0.8 ± 0.1	15.4 ± 0.3
τ + $E_{\mathrm{T}}^{\mathrm{miss}}$	60, 40	2.7 ± 0.1	17.4 ± 0.3
μ + $E_{\mathrm{T}}^{\mathrm{miss}}$	5, 30	0.3 ± 0.1	17.6 ± 0.3
$e\,\gamma$ + $E_{\mathrm{T}}^{\mathrm{miss}}$	15, 30	0.7 ± 0.1	17.7 ± 0.3
μ + jet	7, 100	0.1 ± 0.1	17.8 ± 0.3
$e\,\gamma$ + jet	15, 100	0.6 ± 0.1	17.8 ± 0.3
μ + τ	7, 40	1.2 ± 0.1	18.4 ± 0.3
$e\,\gamma$ + τ	14, 52	5.4 ± 0.2	20.7 ± 0.3
$e\,\gamma$ + μ	15, 7	0.2 ± 0.1	20.7 ± 0.3
Prescaled			22.6 ± 0.3
Total Level-1 Rate			22.6 ± 0.3

Table E.12: The High-Level Trigger Menu at $\mathcal{L} = 2 \times 10^{33}\,\mathrm{cm}^{-2}\,\mathrm{s}^{-1}$ for an output of approximately 120 Hz. The E_{T} values are the kinematic thresholds for the different trigger paths.

Trigger	**Level-1 bits used**	**Level-1 Prescale**	**HLT Threshold (GeV)**	**HLT Rate (Hz)**
Inclusive e	2	1	26	23.5 ± 6.7
e-e	3	1	12, 12	1.0 ± 0.1
Relaxed e-e	4	1	19, 19	1.3 ± 0.1
Inclusive γ	2	1	80	3.1 ± 0.2
γ-γ	3	1	30, 20	1.6 ± 0.7
Relaxed γ-γ	4	1	30, 20	1.2 ± 0.6
Inclusive μ	0	1	19	25.8 ± 0.8
Relaxed μ	0	1	37	11.9 ± 0.5
μ-μ	1	1	7, 7	4.8 ± 0.4
Relaxed μ-μ	1	1	10, 10	8.6 ± 0.6
τ + $E_{\mathrm{T}}^{\mathrm{miss}}$	10	1	65 ($E_{\mathrm{T}}^{\mathrm{miss}}$)	0.5 ± 0.1
Pixel τ-τ	10, 13	1	—	4.1 ± 1.1
Tracker τ-τ	10, 13	1	—	6.0 ± 1.1
τ + e	26	1	52, 16	< 1.0
τ + μ	0	1	40, 15	< 1.0
b-jet (leading jet)	36, 37, 38, 39	1	350, 150, 55 (see text)	10.3 ± 0.3
b-jet (2$^{\mathrm{nd}}$ leading jet)	36, 37, 38, 39	1	350, 150, 55 (see text)	8.7 ± 0.3
Single-jet	36	1	400	4.8 ± 0.0
Double-jet	36, 37	1	350	3.9 ± 0.0
Triple-jet	36, 37, 38	1	195	1.1 ± 0.0
Quadruple-jet	36, 37, 38, 39	1	80	8.9 ± 0.2
$E_{\mathrm{T}}^{\mathrm{miss}}$	32	1	91	2.5 ± 0.2
jet + $E_{\mathrm{T}}^{\mathrm{miss}}$	32	1	180, 80	3.2 ± 0.1
acoplanar 2 jets	36, 37	1	200, 200	0.2 ± 0.0
acoplanar jet + $E_{\mathrm{T}}^{\mathrm{miss}}$	32	1	100, 80	0.1 ± 0.0
2 jets + $E_{\mathrm{T}}^{\mathrm{miss}}$	32	1	155, 80	1.6 ± 0.0
3 jets + $E_{\mathrm{T}}^{\mathrm{miss}}$	32	1	85, 80	0.9 ± 0.1
4 jets + $E_{\mathrm{T}}^{\mathrm{miss}}$	32	1	35, 80	1.7 ± 0.2
Diffractive	Sec. E.3	1	40, 40	< 1.0
H_{T} + $E_{\mathrm{T}}^{\mathrm{miss}}$	31	1	350, 80	5.6 ± 0.2
H_{T} + e	31	1	350, 20	0.4 ± 0.1
Inclusive γ	2	400	23	0.3 ± 0.0
γ-γ	3	20	12, 12	2.5 ± 1.4
Relaxed γ-γ	4	20	19, 19	0.1 ± 0.0
Single-jet	33	10	250	5.2 ± 0.0
Single-jet	34	1 000	120	1.6 ± 0.0
Single-jet	35	100 000	60	0.4 ± 0.0
Total HLT rate				119.3 ± 7.2